Generalized Material Models in TLM—Part 2: Materials with Anisotropic Properties

John Paul, Christos Christopoulos, and David W. P. Thomas, *Member, IEEE*

***Abstract*—Transmission-line modeling (TLM) can be used for the time-domain simulation of electromagnetic wave propagation in anisotropic and bi-anisotropic media. In this paper, $\mathcal{Z}$-transform methods are utilized to obtain the time-domain iteration procedures for propagation in anisotropic and bi-isotropic materials. For clarity, the method is first developed for one-dimensional (1-D) propagation and then extended to the three-dimensional (3-D) case.**

***Index Terms*— Frequency-dependent materials, nonhomogeneous media, time-domain electromagnetics, transmission-line modeling.**

I. Introduction

ANISOTROPIC materials with constant material parameters have been modeled in the finite-difference time-domain (FDTD) method [1]. FDTD was extended to include the frequency-dependent anisotropic material properties of a magnetized plasma [2] and to a magnetized ferrite material [3]. However, because of the offsets between the electric and magnetic fields of half a space-step and half a time-step in a FDTD grid, the resulting update scheme requires spatial and temporal interpolation of fields and as noted in [1] and [2] for three-dimensional (3-D) problems the update scheme is somewhat cumbersome. The main difference between FDTD and transmission-line modeling (TLM) is that in TLM the electric and magnetic fields are solved at the same point in space-time. Thus, it is proposed that TLM is more naturally suited to the modeling of anisotropic and bi-isotropic materials. The modeling of anisotropic materials with constant material parameters in TLM was presented in [4]. The TLM model for propagation in both magnetized plasma and ferrite were developed by Hein [5], [6]. This paper presents an extension of the technique presented for isotropic materials [7] to include frequency-dependent anisotropic and bi-isotropic material properties in the time domain. Although the approach is first developed for one-dimensional (1-D) propagation, the 3-D method follows directly by extension of the 1-D case. The formulation presented here is elegant, efficient, and fits into a unified scheme for dealing with general electromagnetic material properties in the time domain.

Manuscript received July 27, 1999. This work was supported by the Engineering and Physical Sciences Research Council, U.K., and the National Physical Laboratory, U.K., through the funding of a studentship.

The authors are with the Electromagnetics Research Group, School of Electrical and Electronic Engineering, University of Nottingham, Nottingham, NG7 2RD U.K.

Publisher Item Identifier S 0018-926X(99)09848-8.

II. Formulation

A. Maxwell's Equations and the Constitutive Relations

The TLM formulation is developed from Maxwell's curl equations (1) [8]

$$\begin{bmatrix} \nabla \times \underline{H} \\ -\nabla \times \underline{E} \end{bmatrix} = \begin{bmatrix} \underline{J}_e \\ \underline{J}_m \end{bmatrix} + \frac{\partial}{\partial t} \begin{bmatrix} \underline{D} \\ \underline{B} \end{bmatrix}. \tag{1}$$

The constitutive relations for the current and voltage densities are expressed in the following:

$$\begin{bmatrix} \underline{J}_e \\ \underline{J}_m \end{bmatrix} = \begin{bmatrix} \underline{J}_{ef} + \underline{\underline{\sigma}}_e * \underline{E} \\ \underline{J}_{mf} + \underline{\underline{\sigma}}_m * \underline{H} \end{bmatrix}. \tag{2}$$

Equation (3) expresses the constitutive relations for the flux densities. In the general case, the 3×3 material tensors of the constitutive relations describe causal time functions

$$\begin{bmatrix} \underline{D} \\ \underline{B} \end{bmatrix} = \begin{bmatrix} \varepsilon_0 \underline{E} \\ \mu_0 \underline{H} \end{bmatrix} + \begin{bmatrix} \varepsilon_0 \underline{\underline{\chi}}_e & \underline{\underline{\xi}}_r / c \\ \underline{\underline{\zeta}}_r / c & \mu_0 \underline{\underline{\chi}}_m \end{bmatrix} * \begin{bmatrix} \underline{E} \\ \underline{H} \end{bmatrix}. \tag{3}$$

Substitution of (2) and (3) into (1) yields

$$\begin{aligned} \begin{bmatrix} \nabla \times \underline{H} \\ -\nabla \times \underline{E} \end{bmatrix} - \begin{bmatrix} \underline{J}_{ef} \\ \underline{J}_{mf} \end{bmatrix} &= \frac{\partial}{\partial t} \begin{bmatrix} \varepsilon_0 \underline{E} \\ \mu_0 \underline{H} \end{bmatrix} + \begin{bmatrix} \underline{\underline{\sigma}}_e * \underline{E} \\ \underline{\underline{\sigma}}_m * \underline{H} \end{bmatrix} \\ &\quad + \frac{\partial}{\partial t} \begin{bmatrix} \varepsilon_0 \underline{\underline{\chi}}_e & \underline{\underline{\xi}}_r / c \\ \underline{\underline{\zeta}}_r / c & \mu_0 \underline{\underline{\chi}}_m \end{bmatrix} * \begin{bmatrix} \underline{E} \\ \underline{H} \end{bmatrix}. \end{aligned} \tag{4}$$

The TLM model is a discrete time solution of (4), solving for the fields $\underline{E}$ and $\underline{H}$ at each time step.

B. 1-D Formulation

In this section, the TLM formulation for anisotropic and bi-anisotropic materials is presented. For clarity, the development here is presented for the case of 1-D propagation in x, with no coupling to the x-directed field components. In the next section, the approach is extended to the 3-D method based on the symmetrical condensed node (SCN) [9]. Fig. 1 shows the 1-D cell: it has four ports (V_4, V_5, V_{10}, and V_{11}) and four total field quantities (E_y, E_z, H_y, and H_z) which are evaluated at the center of the cell. The curl operations on the left-hand side (LHS) of (4) are solved using Stokes' theorem with integration contours $\mathcal{C}_y$ and $\mathcal{C}_z$ shown in Fig. 1. For consistency with the 3-D development, the port numbers used in the 1-D case are from the 3-D node of Section II-C.

Reduction of (4) to the 1-D case with propagation in x, assuming no coupling from the x component into the y and z

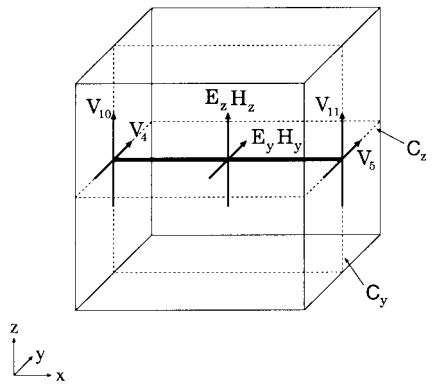

Fig. 1. 1-D anisotropic and bi-anisotropic TLM node.

components and vice versa, and transforming to the frequency domain using $\partial/\partial t \rightarrow s$ gives

$$\begin{bmatrix} (\nabla \times \underline{H})_y \\ (\nabla \times \underline{H})_z \\ -(\nabla \times \underline{E})_y \\ -(\nabla \times \underline{E})_z \end{bmatrix} - \begin{bmatrix} J_{efy} \\ J_{efz} \\ J_{mfy} \\ J_{mfz} \end{bmatrix} = s \begin{bmatrix} \varepsilon_0 E_y \\ \varepsilon_0 E_z \\ \mu_0 H_y \\ \mu_0 H_z \end{bmatrix} + \begin{bmatrix} \underline{\underline{\sigma_e}} & \underline{\underline{\sigma_m}} \end{bmatrix} \cdot \begin{bmatrix} E_y \\ E_z \\ H_y \\ H_z \end{bmatrix} + s \begin{bmatrix} \varepsilon_0 \underline{\underline{\chi_e}} & \underline{\underline{\xi_r}} + /c \\ \underline{\underline{\zeta_r}}/c & \mu_0 \underline{\underline{\chi_m}} \end{bmatrix} \cdot \begin{bmatrix} E_y \\ E_z \\ H_y \\ H_z \end{bmatrix} \tag{5}$$

where for example

$$\underline{\underline{\sigma_e}} = \begin{bmatrix} \sigma_e^{yy} & \sigma_e^{yz} \\ \sigma_e^{zy} & \sigma_e^{zz} \end{bmatrix}, \quad \underline{\underline{\chi_e}} = \begin{bmatrix} \chi_e^{yy} & \chi_e^{yz} \\ \chi_e^{zy} & \chi_e^{zz} \end{bmatrix} \tag{6}$$

and $(\nabla \times \underline{H})_u$ is the component of $\nabla \times \underline{H}$ pointing in u. Using the field-circuit equivalences [7], (5) becomes

$$\begin{bmatrix} V_4 + V_5 \\ V_{10} + V_{11} \\ V_{11} - V_{10} \\ V_4 - V_5 \end{bmatrix} - \begin{bmatrix} i_{fy} \\ i_{fz} \\ V_{fy} \\ V_{fz} \end{bmatrix} = \overline{s} \begin{bmatrix} V_y \\ V_z \\ i_y \\ i_z \end{bmatrix} + \begin{bmatrix} \underline{\underline{g_e}} & \underline{\underline{r_m}} \end{bmatrix} \cdot \begin{bmatrix} V_y \\ V_z \\ i_y \\ i_z \end{bmatrix} + \overline{s} \begin{bmatrix} \underline{\underline{\chi_e}} & \underline{\underline{\xi_r}} \\ \underline{\underline{\zeta_r}} & \underline{\underline{\chi_m}} \end{bmatrix} \cdot \begin{bmatrix} V_y \\ V_z \\ i_y \\ i_z \end{bmatrix}. \tag{7}$$

Converting (7) to the traveling wave format [7] using superscript i to denote incident wave quantities gives

$$2 \begin{bmatrix} V_4 + V_5 \\ V_{10} + V_{11} \\ V_{11} - V_{10} \\ V_4 - V_5 \end{bmatrix}^i - \begin{bmatrix} i_{fy} \\ i_{fz} \\ V_{fy} \\ V_{fz} \end{bmatrix} = 2 \begin{bmatrix} V_y \\ V_z \\ i_y \\ i_z \end{bmatrix} + \begin{bmatrix} \underline{\underline{g_e}} & \underline{\underline{r_m}} \end{bmatrix} \cdot \begin{bmatrix} V_y \\ V_z \\ i_y \\ i_z \end{bmatrix} + \overline{s} \begin{bmatrix} \underline{\underline{\chi_e}} & \underline{\underline{\xi_r}} \\ \underline{\underline{\zeta_r}} & \underline{\underline{\chi_m}} \end{bmatrix} \cdot \begin{bmatrix} V_y \\ V_z \\ i_y \\ i_z \end{bmatrix}. \tag{8}$$

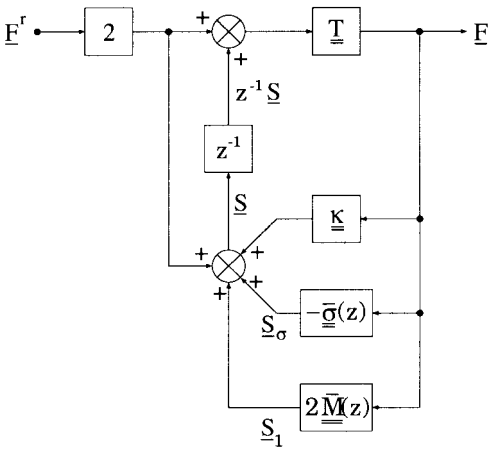

Fig. 2. Signal flow graph for a bi-anisotropic material.

Defining the LHS of this equation as the external excitation

$$2 \begin{bmatrix} V_4 + V_5 \\ V_{10} + V_{11} \\ V_{11} - V_{10} \\ V_4 - V_5 \end{bmatrix}^i - \begin{bmatrix} i_{fy} \\ i_{fz} \\ V_{fy} \\ V_{fz} \end{bmatrix} \equiv 2 \begin{bmatrix} V_y \\ V_z \\ -i_y \\ -i_z \end{bmatrix}^r \tag{9}$$

where the superscript r denotes reflected wave quantities. Equation (8) can be written as

$$2 \begin{bmatrix} \underline{V} \\ -\underline{i} \end{bmatrix}^r = 2 \begin{bmatrix} \underline{V} \\ \underline{i} \end{bmatrix} + \begin{bmatrix} \underline{\underline{g_e}} & \underline{\underline{r_m}} \end{bmatrix} \cdot \begin{bmatrix} \underline{V} \\ \underline{i} \end{bmatrix} + \overline{s} \begin{bmatrix} \underline{\underline{\chi_e}} & \underline{\underline{\xi_r}} \\ \underline{\underline{\zeta_r}} & \underline{\underline{\chi_m}} \end{bmatrix} \cdot \begin{bmatrix} \underline{V} \\ \underline{i} \end{bmatrix}. \tag{10}$$

Equation (10) can be expressed as

$$2\underline{F}^r = (\underline{\underline{2}} + \underline{\underline{\sigma}} + \overline{s}\underline{\underline{M}}) \cdot \underline{F}. \tag{11}$$

Defining a frequency-dependent transmission matrix $\underline{\underline{t}} = 2(\underline{\underline{2}} + \underline{\underline{\sigma}} + \overline{s}\underline{\underline{M}})^{-1}$, (11) becomes

$$\underline{F} = \underline{\underline{t}} \cdot \underline{F}^r. \tag{12}$$

The discrete time-domain model is obtained from (11) using the bilinear $\mathcal{Z}$ transform $\overline{s} = 2(1 - z^{-1})/(1 + z^{-1})$ and the partial fraction expansions

$$(1 + z^{-1})\underline{\underline{\sigma}}(z) = \underline{\underline{\sigma_0}} + z^{-1}(\underline{\underline{\sigma_1}} + \overline{\underline{\sigma}}(z)) \tag{13}$$

$$(1 - z^{-1})\underline{\underline{M}}(z) = \underline{\underline{M_0}} + z^{-1}(\underline{\underline{M_1}} + \overline{\underline{M}}(z)) \tag{14}$$

leading to

$$\underline{\underline{T}}^{-1} \cdot \underline{F} = 2\underline{F}^r + z^{-1}(2\underline{F}^r + \underline{\underline{\kappa}} \cdot \underline{F} - \overline{\underline{\sigma}}(z) \cdot \underline{F} + 2\overline{\underline{M}}(z) \cdot \underline{F}) \tag{15}$$

where $\underline{\underline{T}}^{-1} = \underline{\underline{2}} + \underline{\underline{\sigma_0}} + 2\underline{\underline{M_0}}$ and $\underline{\underline{\kappa}} = -(\underline{\underline{2}} + \underline{\underline{\sigma_1}} - 2\underline{\underline{M_1}})$. Defining the function of the previous time step on the right-hand side of (15) as the main accumulator vector $\underline{S}$, the update scheme for the total fields is

$$\underline{F} = \underline{\underline{T}} \cdot (2\underline{F}^r + z^{-1}\underline{S}). \tag{16}$$

The process described by (16) is illustrated by the signal flow diagram of Fig. 2. This figure shows the detail of the block $\underline{\underline{t}}(z)$ required in [7, fig. 4] for modeling anisotropic and bi-anisotropic material properties.

C. 3-D Formulation

Before discussion of the 3-D method, the iteration process of the 1-D node developed in the previous section is summarized. The TLM scattering process consists of three steps. In the first step of (17), the curls of the incident voltages and the free-source excitations are evaluated, in the second step of (18), the total fields are calculated using the recursive convolution process described by the transmission matrix $\underline{\underline{t}}$. In the final step of (19), the reflected voltages are calculated from the total fields and incident voltages. Note that for general material modeling, only the process described by matrix $\underline{\underline{t}}$ needs to be modified. This system is represented by the flow diagram shown in [7, fig. 4]

$$\begin{bmatrix} V_y \\ V_z \\ -i_y \\ -i_z \end{bmatrix}^r = \begin{bmatrix} V_4+V_5 \\ V_{10}+V_{11} \\ V_{11}-V_{10} \\ V_4-V_5 \end{bmatrix}^i - \tfrac{1}{2}\begin{bmatrix} i_{fy} \\ i_{fz} \\ V_{fy} \\ V_{fz} \end{bmatrix} \tag{17}$$

$$\begin{bmatrix} V_y \\ V_z \\ i_y \\ i_z \end{bmatrix}^r = \underline{\underline{t}} \cdot \begin{bmatrix} V_y \\ V_z \\ i_y \\ i_z \end{bmatrix}^r \tag{18}$$

$$\begin{bmatrix} V_4 \\ V_5 \\ V_{10} \\ V_{11} \end{bmatrix}^r = \begin{bmatrix} V_y - i_z - V_5^i \\ V_y + i_z - V_4^i \\ V_z + i_y - V_{11}^i \\ V_z - i_y - V_{10}^i \end{bmatrix}. \tag{19}$$

The basic element of the 3-D TLM method is the symmetrical condensed node (SCN) shown in [7, fig. 3]. The iteration process is identical to that detailed in [7, eq. (16), (18), and (20)], with the matrix $\underline{\underline{t}}(z)$ now a full 6×6 matrix. The iteration procedure is of the same form developed above for the 1-D case. The speed of propagation on the transmission-lines of a 3-D mesh is $2c = \Delta\ell/\Delta t$, thus, in the 3-D case, (11) is modified to

$$2\underline{F}^r = (\underline{\underline{4}} + \underline{\underline{\sigma}} + \overline{s}2\underline{\underline{M}}) \cdot \underline{F}. \tag{20}$$

III. Frequency-Dependent Materials

A. Magnetized Plasma

From the equation of motion of an electron plasma subject to a static bias magnetization $\underline{B}_0$, the differential equation governing the conduction current density is [8], [5]

$$\frac{\partial \underline{J}_{ec}}{\partial t} + \nu_c\, \underline{J}_{ec} = \frac{N\, q^2}{m}\, \underline{E} + \underline{J}_{ec} \times \underline{\omega}_b \tag{21}$$

where ν_c is the collision frequency, N is number density of electrons, q is the electron charge, m is the electron mass and the cyclotron frequency vector $\underline{\omega}_b = \underline{B}_0 q/m$. The Laplace transform of (21) is

$$(s+\nu_c)\underline{J}_{ec} = \frac{Nq^2}{m}\, \underline{E} + \underline{J}_{ec} \times \underline{\omega}_b. \tag{22}$$

By taking the dot product and cross product with $\underline{\omega}_b$ of (22) gives

$$\underline{J}_{ec} = \frac{Nq^2}{m}\left[\frac{s+\nu_c}{(s+\nu_c)^2+\omega_b^2}\,\underline{E} - \frac{1}{(s+\nu_c)^2+\omega_b^2}\,(\underline{\omega}_b \times \underline{E}) + \frac{1}{(s+\nu_c)\left((s+\nu_c)^2+\omega_b^2\right)}\,\underline{\omega}_b\underline{\omega}_b \cdot \underline{E}\right]. \tag{23}$$

For the bias field in x, (23) becomes

$$\underline{J}_{ec} = \begin{bmatrix} \dfrac{\sigma_{e0}\nu_c}{s+\nu_c} & & \\ & \dfrac{\sigma_{e0}\nu_c(s+\nu_c)}{(s+\nu_c)^2+\omega_b^2} & \dfrac{\sigma_{e0}\nu_c\omega_b}{(s+\nu_c)^2+\omega_b^2} \\ & -\dfrac{\sigma_{e0}\nu_c\omega_b}{(s+\nu_c)^2+\omega_b^2} & \dfrac{\sigma_{e0}\nu_c(s+\nu_c)}{(s+\nu_c)^2+\omega_b^2} \end{bmatrix} \cdot \underline{E} = \underline{\underline{\sigma_e}} \cdot \underline{E} \tag{24}$$

using static conductivity $\sigma_{e0} = Nq^2/m\nu_c$. Reducing to the 1-D example with propagation in x gives the elements of the electric conductivity tensor $\underline{\underline{\sigma_e}}$ of (5) for description of a magnetized plasma. Using $\underline{\underline{g_e}} = \eta_0 \Delta\ell \underline{\underline{\sigma_e}}$ and $g_{e0} = \eta_0 \Delta\ell \sigma_{e0}$ gives the normalized electric conductivity tensor

$$\underline{\underline{g_e}} = \frac{g_{e0}\,\nu_c}{(s+\nu_c)^2+\omega_b^2}\begin{bmatrix} s+\nu_c & \omega_b \\ -\omega_b & s+\nu_c \end{bmatrix} = \begin{bmatrix} g_e^{yy} & g_e^{yz} \\ g_e^{zy} & g_e^{zz} \end{bmatrix}. \tag{25}$$

The elements of this tensor are second-order functions of frequency and as shown in [10], an efficient technique for the solution of second-order functions involves a complex recursive convolution, with the real part ($\Re$) of the complex accumulator used in the update of the total fields. The components of $\underline{\underline{g_e}}$ can be written as the real part of two complex first-order functions, i.e.

$$g_e^{yy}(s) = g_e^{zz}(s) = g_{e0}\,\nu_c \frac{s+\nu_c}{(s+\nu_c)^2+\omega_b^2} = g_{e0}\,\nu_c\,\Re\left[\frac{1}{s+(\nu_c - j\omega_b)}\right] \tag{26}$$

$$g_e^{yz}(s) = -g_e^{zy}(s) = g_{e0}\,\nu_c \frac{\omega_b}{(s+\nu_c)^2+\omega_b^2} = g_{e0}\,\nu_c\,\Re\left[\frac{-j}{s+(\nu_c - j\omega_b)}\right]. \tag{27}$$

The impulse invariant $\mathcal{Z}$ transforms of (26) and (27) are

$$g_e^{yy}(z) = g_e^{zz}(z) = g_{e0}\nu_c\Re\left[\frac{\dfrac{1-\beta_p}{\nu_c - j\omega_b}}{1-z^{-1}\beta_p}\right]$$

$$g_e^{yz}(z) = -g_e^{zy}(z) = g_{e0}\nu_c\Re\left[\frac{\dfrac{-j(1-\beta_p)}{\nu_c - j\omega_b}}{1-z^{-1}\beta_p}\right]. \tag{28}$$

The conductivity tensor in the $\mathcal{Z}$ domain is

$$\underline{\underline{g_e}}(z) = g_{e0}\nu_c\Re\left(\frac{1-\beta_p}{\nu_c - j\omega_b}\begin{bmatrix} 1 & -j \\ j & 1 \end{bmatrix}\right) \tag{29}$$

using $\beta_p = e^{-(\nu_c - j\omega_b)\Delta t}$. Assuming the background permittivity is that of free-space, i.e., $\underline{\underline{\chi_e}} = \underline{\underline{0}}$, the $\mathcal{Z}$ transform of the top line of (10) is

$$2\underline{V}^r = (\underline{\underline{2}} + \underline{\underline{g_e}}(z)) \cdot \underline{V}. \tag{30}$$

For a causal function $\underline{\underline{g_e}}$, which is exponential in nature (i.e., can be solved recursively) it is always possible to take a partial fraction expansion to obtain a constant tensor $\underline{\underline{g_{e0}}}$ and a

frequency-dependent tensor $\underline{\underline{g_e}}(z)$, which is a function of the previous time step, i.e.,

$$\underline{\underline{g_e}}(z) = \underline{\underline{g_{e0}}} + z^{-1}\underline{\underline{g_e}}(z). \tag{31}$$

Substitution of (31) into (30) and manipulating gives

$$(\underline{\underline{2}} + \underline{\underline{g_{e0}}}) \cdot \underline{V} = 2\underline{V}^r - z^{-1}\underline{\underline{g_e}}(z) \cdot \underline{V}. \tag{32}$$

The matrix $\underline{\underline{T_e}}^{-1} = \underline{\underline{2}} + \underline{\underline{g_{e0}}}$ contains constant elements and, thus, $\underline{\underline{T_e}}$ can be found, leading to the iteration process

$$\underline{V} = \underline{\underline{T_e}} \cdot (2\underline{V}^r - z^{-1}\underline{\underline{g_e}}(z) \cdot \underline{V}). \tag{33}$$

Taking the partial fraction expansion of (29) as in (31) gives

$$\underline{\underline{g_{e0}}} = \begin{bmatrix} g_{e0}^{yy} & g_{e0}^{yz} \\ g_{e0}^{zy} & g_{e0}^{zz} \end{bmatrix} = g_{e0}\,\nu_c\,\Re\left(\frac{1-\beta_p}{\nu_c - j\omega_b}\begin{bmatrix} 1 & -j \\ j & 1 \end{bmatrix}\right) \tag{34}$$

and defining $\alpha_p = g_{e0}\nu_c(1-\beta_p)\beta_p/(\nu_c - j\omega_b)$

$$\underline{\underline{g_e}}(z) = \Re\left(\frac{\alpha_p}{1 - z^{-1}\beta_p}\begin{bmatrix} 1 & -j \\ j & 1 \end{bmatrix}\right). \tag{35}$$

Inverting the matrix $\underline{\underline{T_e}}^{-1}$ gives

$$\underline{\underline{T_e}} = \frac{1}{(2+g_{e0}^{yy})(2+g_{e0}^{zz}) - g_{e0}^{yz}g_{e0}^{zy}}\begin{bmatrix} 2+g_{e0}^{zz} & -g_{e0}^{yz} \\ -g_{e0}^{zy} & 2+g_{e0}^{yy} \end{bmatrix}. \tag{36}$$

Declaring an accumulator vector $\underline{S_e} = \underline{\underline{g_e}}(z) \cdot \underline{V}$, (33) is

$$\underline{V} = \underline{\underline{T_e}} \cdot (2\underline{V}^r - z^{-1}\underline{S_e}). \tag{37}$$

In this method, the convolution is complex with the real part of $\underline{S_e}$ used in the total field update. In full, the total field update equation for the 1-D case is

$$\begin{bmatrix} V_y \\ V_z \end{bmatrix} = \underline{\underline{T_e}} \cdot \left(2\begin{bmatrix} V_y \\ V_z \end{bmatrix}^r - z^{-1}\,\Re\begin{bmatrix} S_{ey} \\ S_{ez} \end{bmatrix}\right). \tag{38}$$

The accumulator update is

$$\begin{bmatrix} S_{ey} \\ S_{ez} \end{bmatrix} = \alpha_p\begin{bmatrix} 1 & -j \\ j & 1 \end{bmatrix} \cdot \begin{bmatrix} V_y \\ V_z \end{bmatrix} + z^{-1}\beta_p\begin{bmatrix} S_{ey} \\ S_{ez} \end{bmatrix}. \tag{39}$$

The matrix in (39) indicates the expected Faraday rotation of a linearly polarized wave traveling through a magnetized plasma. This algorithm requires the storage of one real and one complex number (i.e., three real numbers) per electric field component.

IV. Magnetized Ferrite

The modeling of a magnetized ferrite follows from a similar approach to the previous model of propagation in magnetized plasma. The damping in ferrite media is introduced phenomenologically [11], leading to two distinct forms of the equation of motion of the magnetization vector. In the Landau–Lifshitz form, the equation of motion is

$$\frac{\partial \underline{M}}{\partial t} = -\gamma(\underline{M} \times \underline{H}) - \frac{\gamma\alpha}{|\underline{M}|}(\underline{M} \times (\underline{M} \times \underline{H})). \tag{40}$$

By taking the cross product with $\underline{M}$ and neglecting small terms, (40) becomes Gilbert's equation of motion, i.e.

$$\frac{\partial \underline{M}}{\partial t} = -\gamma(\underline{M} \times \underline{H}) + \frac{\gamma\alpha}{|\underline{M}|}\left(\underline{M} \times \frac{\partial \underline{M}}{\partial t}\right). \tag{41}$$

Alternatively, in the Bloch–Bloembergen form the equation of motion is

$$\frac{\partial \underline{M}_{tr}}{\partial t} = -\gamma(\underline{M} \times \underline{H})_{tr} - \nu_s\underline{M}_{tr}. \tag{42}$$

In (40)–(42), $\underline{M}$ is the magnetization vector, γ is the gyromagnetic ratio, α is a dimensionless damping parameter, subscript $_{tr}$ denotes the vector quantity transverse to the bias fields and ν_s is the transverse relaxation frequency. Assuming the magnetization vector and the magnetic field vector have the form

$$\underline{H} = \underline{H_0} + \underline{h}, \underline{M} = \underline{M_0} + \underline{m} \tag{43}$$

where $\underline{H_0}$ is the static bias field, $\underline{M_0}$ is the saturation magnetization, $\underline{h}$ is the time-varying magnetic field vector and $\underline{m}$ is the time-varying magnetization vector. Furthermore, by assuming small-signal conditions $\underline{M_0} \gg \underline{m}$, $\underline{H_0} \gg \underline{h}$ and that the bias field vectors $\underline{M_0}$ and $\underline{H_0}$ point in the x direction, the cross products in (41) and (42) can be approximated as

$$\begin{aligned} \underline{M} \times \underline{H} \sim\ & -\underline{\hat{y}}(M_0h_z - H_0m_z) \\ & +\underline{\hat{z}}(M_0h_y - H_0m_y) \end{aligned} \tag{44}$$

$$\underline{M} \times \frac{\partial \underline{M}}{\partial t} \sim\ -\underline{\hat{y}}M_0\frac{\partial m_z}{\partial t} + \underline{\hat{z}}M_0\frac{\partial m_y}{\partial t}. \tag{45}$$

Defining the precessional frequency $\omega_0 = \gamma H_0$ and magnetization frequency $\omega_m = \gamma M_0$, both Gilbert's equation (41) and Bloch's equation (42) lead to expressions connecting the magnetization with the magnetic field

$$\begin{bmatrix} m_y \\ m_z \end{bmatrix} = \begin{bmatrix} \chi_m^{yy} & \chi_m^{yz} \\ \chi_m^{zy} & \chi_m^{zz} \end{bmatrix} \cdot \begin{bmatrix} h_y \\ h_z \end{bmatrix}, \quad \underline{m} = \underline{\underline{\chi_m}} \cdot \underline{h} \tag{46}$$

where the susceptibility tensor from Gilbert's equation is

$$\underline{\underline{\chi_m}} = \frac{\omega_m}{s^2 + (s\alpha + \omega_0)^2}\begin{bmatrix} s\alpha + \omega_0 & s \\ -s & s\alpha + \omega_0 \end{bmatrix} \tag{47}$$

and the susceptibility tensor from Bloch's equation is

$$\underline{\underline{\chi_m}} = \frac{\omega_m}{(s+\nu_s)^2 + \omega_0^2}\begin{bmatrix} \omega_0 & s+\nu_s \\ -(s+\nu_s) & \omega_0 \end{bmatrix}. \tag{48}$$

A. Bloch Damping

The model of propagation in magnetized ferrite with the Bloch damping term follows from the $\mathcal{Z}$ transform of (48), i.e.,

$$\underline{\underline{\chi_m}}(z) = \omega_m\,\Re\left(\frac{\dfrac{1-\beta_m}{\nu_s - j\omega_0}}{1 - z^{-1}\beta_m}\begin{bmatrix} -j & 1 \\ -1 & -j \end{bmatrix}\right). \tag{49}$$

As in (14), the model is found by the expansion

$$(1 - z^{-1})\underline{\underline{\chi_m}}(z) = \underline{\underline{\chi_{m0}}} - z^{-1}\underline{\underline{\chi_m}}(z). \tag{50}$$

This step leads to the matrix of coefficients

$$\underline{\underline{\chi_{m0}}} = \omega_m\,\Re\left(\frac{1-\beta_m}{\nu_s - j\omega_0}\begin{bmatrix} -j & 1 \\ -1 & -j \end{bmatrix}\right) \tag{51}$$

and the recursive convolution function

$$\underline{\underline{\overline{\chi_m}}}(z) = \omega_m \, \Re\left(\frac{(1-\beta_m)^2}{\nu_s - j\omega_0} \frac{\begin{bmatrix} -j & 1 \\ -1 & -j \end{bmatrix}}{1 - z^{-1}\beta_m} \right). \quad (52)$$

From the bottom line of (10), the update equation for a frequency-dependent anisotropic magnetic medium is

$$(\underline{\underline{2}} + 2\underline{\underline{\chi_{m0}}}) \cdot \underline{i} = -2\underline{i}^{\,r} + z^{-1}[-2\underline{i}^{\,r} - 2\underline{i} + 2\underline{\underline{\overline{\chi_m}}}(z) \cdot \underline{i}]. \quad (53)$$

Defining $\alpha_m = 2\omega_m(1-\beta_m)^2/(\nu_s - j\omega_0)$ and accumulator vector $\underline{S_{m1}}$ where

$$\underline{S_{m1}} = \frac{\alpha_m}{1 - z^{-1}\beta_m} \begin{bmatrix} -j & 1 \\ -1 & -j \end{bmatrix} \cdot \begin{bmatrix} i_y \\ i_z \end{bmatrix}. \quad (54)$$

Equation (53) can be written as

$$(\underline{\underline{2}} + 2\underline{\underline{\chi_{m0}}}) \cdot \underline{i} = -2\underline{i}^{\,r} + z^{-1}(-2\underline{i}^{\,r} - 2\underline{i} + \Re[\underline{S_{m1}}]). \quad (55)$$

Defining matrix $\underline{\underline{T_m}}^{-1} = (\underline{\underline{2}} + 2\underline{\underline{\chi_{m0}}})$ and main accumulator $\underline{S_m} = -2\underline{i}^{\,r} - 2\underline{i} + \Re[\underline{S_{m1}}]$, the iteration scheme is

$$\underline{i} = \underline{\underline{T_m}} \cdot (-2\underline{i}^{\,r} + z^{-1}\underline{S_m}). \quad (56)$$

B. Gilbert Damping

To include the Gilbert damping term in a model of propagation in a magnetized ferrite, it is necessary to take the $\mathcal{Z}$ transform of (47), i.e.,

$$\underline{\underline{\chi_m}}(z) = \frac{\omega_m}{\omega_0} \, \Re\left(\frac{1-\beta_m}{1 - z^{-1}\beta_m} \begin{bmatrix} 1 & j \\ -j & 1 \end{bmatrix} \right). \quad (57)$$

The expansion $(1-z^{-1})\underline{\underline{\chi_m}}(z) = \underline{\underline{\chi_{m0}}} - z^{-1}\underline{\underline{\overline{\chi_m}}}(z)$ gives the coefficient matrix

$$\underline{\underline{\chi_{m0}}} = \frac{\omega_m}{\omega_0} \, \Re\left((1-\beta_m) \begin{bmatrix} 1 & j \\ -j & 1 \end{bmatrix} \right) \quad (58)$$

and the recursive convolution function

$$\underline{\underline{\overline{\chi_m}}}(z) = \frac{\omega_m}{\omega_0} \, \Re\left(\frac{(1-\beta_m)^2}{1 - z^{-1}\beta_m} \begin{bmatrix} 1 & j \\ -j & 1 \end{bmatrix} \right). \quad (59)$$

The iteration procedure follows by a similar development to that given for Bloch damping, i.e., by defining $\alpha_m = 2\omega_m(1-\beta_m)^2/\omega_0)$ and accumulator vector $\underline{S_{m1}}$ where

$$\underline{S_{m1}} = \frac{\alpha_m}{1 - z^{-1}\beta_m} \begin{bmatrix} 1 & j \\ -j & 1 \end{bmatrix} \cdot \begin{bmatrix} i_y \\ i_z \end{bmatrix}. \quad (60)$$

Both models of a magnetized ferrite require the storage of one real and one complex number per magnetic field component.

V. Bi-Isotropic Medium

For simplicity, consider a bi-isotropic material [12], i.e., the susceptibility and magnetoelectric coupling tensors of (3) have the form

$$\underline{\underline{\chi_e}} = \chi_e \underline{\underline{1}}, \underline{\underline{\chi_m}} = \chi_m \underline{\underline{1}}, \underline{\underline{\xi_r}} = \xi_r \underline{\underline{1}}, \underline{\underline{\zeta_r}} = \zeta_r \underline{\underline{1}} \quad (61)$$

where $\underline{\underline{1}}$ is the unit matrix. Furthermore, in a chiral bi-isotropic medium, e.g., an artificial material constructed by a dispersal of scatterers in a background material, to a first approximation the effective material parameters are Lorentzian (second-order) in form [12]. The electric susceptibility is given by

$$\chi_e(s) = \frac{\chi_{e0}\omega_0^2}{s^2 + s2\delta + \omega_0^2} \quad (62)$$

where χ_{e0} is the dc electric susceptibility, ω_0 is the resonant frequency, and δ is the damping frequency. The magnetic susceptibility is given by

$$\chi_m(s) = -\frac{\chi_{m\infty}s^2}{s^2 + s2\delta + \omega_0^2} \quad (63)$$

where $\chi_{m\infty}$ is the magnetic susceptibility at high frequencies. The frequency dependence of the magnetoelectric coupling parameters obey the one resonance Condon model [12], [13]

$$\xi_r(s) = -\zeta_r(s) = \frac{s\tau\omega_0^2}{s^2 + s2\delta + \omega_0^2} \quad (64)$$

where τ is the chirality time constant. In this case, (10) is reduced to

$$2\begin{bmatrix} V_y \\ V_z \\ -i_y \\ -i_z \end{bmatrix}^r = 2\begin{bmatrix} V_y \\ V_z \\ i_y \\ i_z \end{bmatrix} + \overline{s}\begin{bmatrix} \chi_e & & \xi_r & \\ & \chi_e & & \xi_r \\ -\xi_r & & \chi_m & \\ & -\xi_r & & \chi_m \end{bmatrix} \cdot \begin{bmatrix} V_y \\ V_z \\ i_y \\ i_z \end{bmatrix}. \quad (65)$$

As in (10), expressing (65) in matrix form gives

$$2\begin{bmatrix} \underline{V} \\ -\underline{i} \end{bmatrix}^r = \left(\underline{\underline{2}} + \overline{s}\begin{bmatrix} \chi_e & \xi_r \\ -\xi_r & \chi_m \end{bmatrix} \right) \cdot \begin{bmatrix} \underline{V} \\ \underline{i} \end{bmatrix}. \quad (66)$$

Applying the bilinear $\mathcal{Z}$ transform to (66) gives (in shorthand form)

$$2(1+z^{-1})\underline{F}^r = 2(1+z^{-1})\underline{F} + 2(1-z^{-1})\underline{\underline{M}} \cdot \underline{F}. \quad (67)$$

Utilizing the transforms of the second-order functions in (26)–(28) in (62)–(64) gives the $\mathcal{Z}$ transforms of the material parameters

$$\chi_e(z) = \Re\left[\frac{(1-\beta_c)C_e}{1 - z^{-1}\beta_c}\right], \quad \chi_m(z) = \Re\left[\frac{(1-\beta_c)C_m}{1 - z^{-1}\beta_c}\right]$$
$$\xi_r(z) = \Re\left[\frac{(1-\beta_c)C_c}{1 - z^{-1}\beta_c}\right] \quad (68)$$

where $\beta = \sqrt{\omega_0^2 - \delta^2}$ and $\beta_c = e^{-(\delta - j\beta)\Delta t}$, the complex coefficients are

$$C_e = \chi_{e0}\left(1 - j\frac{\delta}{\beta}\right), \quad C_m = \chi_{m\infty}\left(1 + j\frac{\delta}{\beta}\right)$$
$$C_c = j\frac{\tau\omega_0^2}{\beta}.$$

As in previous examples, performing the time differencing and partial fraction expansion of these functions gives, for example

$$(1-z^{-1})\chi_e(z) = \Re[(1-\beta_c)C_e] - z^{-1}\,\Re\left[\frac{(1-\beta_c)^2 C_e}{1-z^{-1}\beta_c}\right] = \chi'_{e0} - z^{-1}\overline{\chi_e}(z) \tag{69}$$

with similar expressions for $(1-z^{-1})\chi_m(z)$ and $(1-z^{-1})\xi(z)$. Substitution of these into (67) yields

$$\underline{\underline{T}}^{-1}\cdot\underline{F} = 2(1-z^{-1})\underline{F}^r + z^{-1}2\underline{F} + 2\underline{\underline{M}}\cdot\underline{F} \tag{70}$$

where

$$\underline{\underline{T}}^{-1} = \begin{bmatrix} 2+2\chi'_{e0} & 2\xi_{r0} \\ -2\xi_{r0} & 2+\chi_{m0} \end{bmatrix}$$
$$\underline{\underline{M}}(z) = \begin{bmatrix} \overline{\chi_e}(z) & \overline{\xi_r}(z) \\ -\overline{\xi_r}(z) & \overline{\chi_m}(z) \end{bmatrix}.$$

The iteration process is

$$\underline{F} = \underline{\underline{T}}\cdot(2\underline{F}^r + z^{-1}\underline{S}) \tag{71}$$

where $\underline{S} = 2\underline{F}^r + 2\underline{F} + \Re[\underline{S}_1]$ and $\underline{S}_1 = 2\underline{\underline{M}}(z)\cdot\underline{F}$ as shown in Fig. 2. Defining $\alpha_c = 2(1-\beta_c)^2$, the accumulator update equation is

$$\underline{S}_1 = \frac{\alpha_c}{1-z^{-1}\beta_c}\begin{bmatrix} C_e & C_c \\ -C_c & C_m \end{bmatrix}\cdot\underline{F}. \tag{72}$$

Thus, the TLM model of a bi-isotropic material requires the storage of one real and one complex number per field component.

VI. Results

In this section, results are presented for propagation in anisotropic and bi-isotropic materials.

A. Magnetized Plasma

One example of a frequency-dependent anisotropic conductive material is a magnetized plasma. Following the example of [2], the reflection and transmission coefficients for a slab of magnetized plasma was calculated using TLM. The slab had depth 9 mm, the space-step $\Delta\ell = 75$ μm, and the time step was $\Delta t = \Delta\ell/c$. In the FDTD formulation a time-step $\Delta t = \Delta\ell/(2c)$ was required for stability, whereas the TLM model was stable at the free-space time-step. After launching a delta function at the slab, the copolarized and cross-polarized reflected and transmitted electric fields were saved for transformation to the frequency-domain. Assuming the incident wave was linearly polarized in z, the transmission coefficients for left-hand circularly polarized (LCP) and right-hand circularly polarized (RCP) waves were obtained using

$$T_{RCP} = E_y^t(\omega) + jE_z^t(\omega)$$
$$T_{LCP} = E_y^t(\omega) - jE_z^t(\omega). \tag{73}$$

The reflection coefficients were calculated with similar expressions involving the reflected fields.

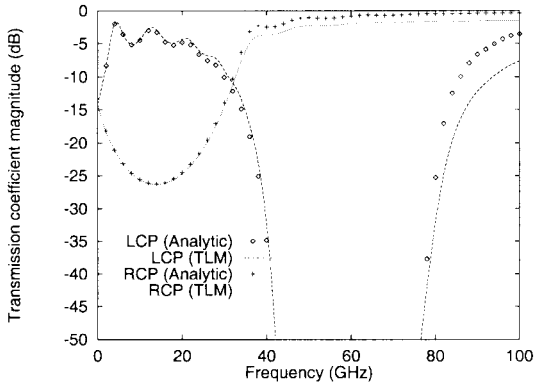

Fig. 3. Frequency-domain transmission coefficients of the magnetized plasma slab.

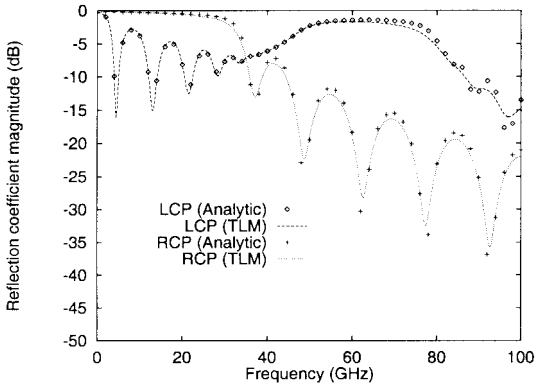

Fig. 4. Frequency-domain reflection coefficients of the magnetized plasma slab.

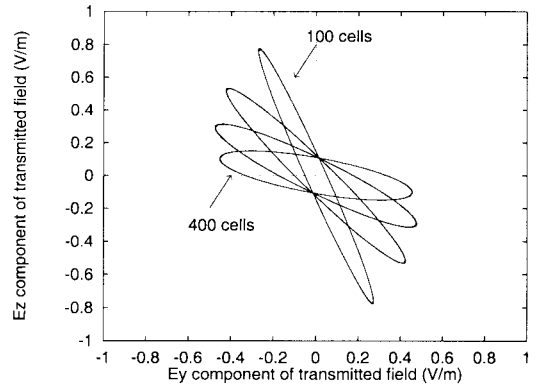

Fig. 5. Faraday rotation in a magnetized plasma.

B. Magnetized Ferrite

Based on the FDTD simulation of 1-D propagation in a magnetized ferrite [3], the reflection and transmission coefficient of a slab of this material was obtained using TLM. The space-step was 75 μm, the time-step was $\Delta t = \Delta\ell/c$, the slab had a depth of 25 cells and had background parameters $\varepsilon_r = \mu_r = 2$. For the model of Gilbert damping, the ferrite parameters were $\omega_0 = \omega_m = 2\pi \times 20 \times 10^9$ and $\alpha = 0.1$. The parameters selected for the model of Bloch damping were $\omega_0 = 2\pi \times 19.8 \times 10^9$, $\omega_m = 2\pi \times 20.2 \times 10^9$, and $\nu_c = 2\pi \times 1.98 \times 10^9$. Figs. 6 and 7 compare the

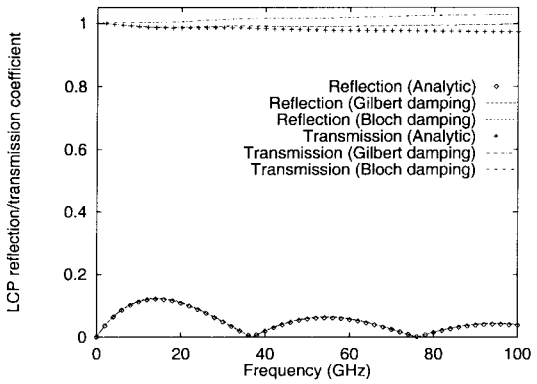

Fig. 6. LCP transmission and reflection coefficients.

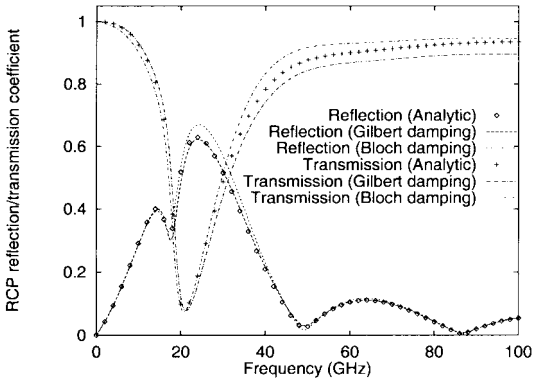

Fig. 7. RCP transmission and reflection coefficient.

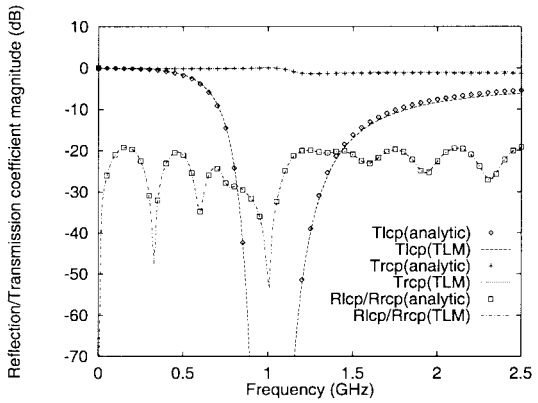

Fig. 8. Transmission and reflection coefficients of a chiral slab.

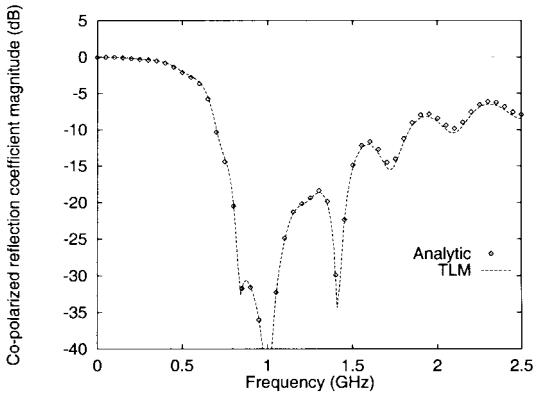

Fig. 9. Copolarized reflection coefficient of a metal backed chiral slab.

reflection and transmission performance of the slab obtained using TLM with the analytic solution for Gilbert damping [15]. As shown, both the Bloch and Gilbert damping methods gave similar performance. In agreement with the discussion in [11], the analytical (not shown) and numerical solutions for the transmission coefficient of LCP waves in the Bloch damped ferrite slab were found to be greater than one. Because the magnetized ferrite is a passive material, this indicates a limitation of the Bloch model.

C. Bi-Isotropic Medium

Finally, as an example of propagation in a chiral material, the reflection and transmission coefficients of a slab were obtained using TLM and frequency domain analysis [12]. The properties were $\chi_{e0} = \chi_{m\infty} = \omega_0\tau = 0.5$, resonant frequency $\omega_0 = 2\pi \times 1000 \times 10^6$, and damping frequency $\delta = 2\pi \times 100 \times 10^6$. The background relative permittivity and permeability of the slab were selected as $\varepsilon_r = \mu_r = 2$. The simulation space-step was $\Delta\ell = 1$ mm and the slab thickness was 200 mm. Fig. 8 shows the analytic and TLM solutions for the transmission and reflection coefficients of the structure for circularly polarized waves. The transmission/reflection response is similar to the magnetized ferrite, indicating an application of chiral materials as microwave isolators.

To examine the absorbing performance, the slab was terminated with a metal backing and the simulation repeated. Fig. 9 shows the copolarized reflection coefficient for this case, indicating that chiral materials may be employed as absorbing structures.

VII. Conclusion

In this paper, the iteration schemes for the time-domain modeling of propagation in frequency-dependent anisotropic and bi-isotropic materials have been developed. Although for clarity the analysis has concentrated on the 1-D scheme, it has been shown that the 3-D case follows directly by simply increasing the order of the matrices and vectors of the 1-D case. Results have been presented for propagation in magnetized plasma and magnetized ferrite media and the TLM solution has been found to be stable, yielding results which correlate with the analytic solutions. Finally, a chiral material has been modeled in the time-domain showing that TLM can be applied to materials that display magnetoelectric coupling.

References

[1] J. Schneider and S. Hudson, "The finite-difference time-domain method applied to anisotropic material," *IEEE Trans. Antennas Propagat.*, vol. 41, pp. 994–999, July 1993.

[2] F. Hunsberger, R. Luebbers, and K. Kunz, "Finite-difference time-domain analysis of gyrotropic media—Part I: Magnetized plasma," *IEEE Trans. Antennas Propagat.*, vol. 40, pp. 1489–1495, Dec. 1992.

[3] K. S. Kunz and R. J. Luebbers, *The Finite Difference Time Domain Method for Electromagnetics*. Boca Raton, FL: CRC, 1993.

[4] L. de Menezes and W. J. R. Hoefer, "Modeling of general constitutive relationships using SCN TLM," *IEEE Trans. Microwave Theory Tech.*, vol. 44, pp. 854–861, June 1996.

[5] S. Hein, "Synthesis of TLM algorithms in the propagator integral framework," in *2nd Int. Workshop Transmission-Line Matrix (TLM) Modeling Theory Applicat.*, Tech. Univ., Munich, Germany, Oct. 1997, pp. 1–11.
[6] ———, "TLM numerical solution of Bloch's equations for magnetized gyrotropic media," *Appl. Math. Modeling*, vol. 21, pp. 221–229, Apr. 1997.
[7] J. Paul, C. Christopoulos, and D. W. P. Thomas, "Generalized material models in TLM—Part 1: Materials with frequency-dependent properties," *IEEE Trans. Antennas Propagat.*, this issue, pp. 1528–1534.
[8] J. A. Kong. *Electromagnetic Wave Theory*. New York: Wiley, 1986.
[9] P. B. Johns, "A symmetrical condensed node for the TLM method," *IEEE Trans. Microwave Theory Tech.*, vol. 35, pp. 370–377, Apr. 1987.
[10] R. J. Luebbers and F. Hunsberger, "FDTD for nth-order dispersive media," *IEEE Trans. Antennas Propagation*, vol. 40, pp. 1297–1301, Nov. 1992.
[11] S. V. Vonsovskii. *Ferromagnetic Resonance*. New York: Pergamon, 1966.
[12] I. V. Lindell, A. H. Sihvola, S. A. Tretyakov, and A. J. Viitanen, *Electromagnetic Waves in Chiral and Bi-Isotropic Media*. Norwood MA: Artech House, 1994.
[13] A. H. Sihvola, "Temporal dispersion in chiral composite materials: A theoretical study," *J. Electromagn. Waves Applicat.*, vol. 6, pp. 1177–1196, 1993.
[14] V. L. Ginzburg. *The Propagation of Electromagnetic Waves in Plasmas*. New York: Pergamon, 1970.
[15] B. Lax and K. J. Button. *Microwave Ferrites and Ferrimagnetics*. New York: McGraw-Hill, 1962.

John Paul, for a photograph and biography, see this issue, p. 1534.

Christos Christopoulos, for a photograph and biography, see this issue, p. 1534.

David W. P. Thomas (M'95), for photograph and biography, see this issue, p. 1534.